

## Magnetocrystalline anisotropy and first-order magnetisation processes in $(\text{Pr}_{1-x}\text{Nd}_x)_2\text{Fe}_{14}\text{B}$ compounds

This article has been downloaded from IOPscience. Please scroll down to see the full text article.

1990 J. Phys.: Condens. Matter 2 7317

(<http://iopscience.iop.org/0953-8984/2/35/007>)

View [the table of contents for this issue](#), or go to the [journal homepage](#) for more

Download details:

IP Address: 171.66.16.103

The article was downloaded on 11/05/2010 at 06:05

Please note that [terms and conditions apply](#).

## Magnetocrystalline anisotropy and first-order magnetisation processes in $(\text{Pr}_{1-x}\text{Nd}_x)_2\text{Fe}_{14}\text{B}$ compounds

G Marusi†, N V Mushnikov‡, L Pareti†, M Solzi† and A E Ermakov‡

† Istituto MASPEC, via Chiavari 18/A, 43100 Parma, Italy

‡ Institute of Metal Physics, Academy of Sciences, 620083 Sverdlovsk, USSR

Received 7 July 1989, in final form 5 March 1990

**Abstract.** The magnetocrystalline anisotropy of the pseudobinary  $(\text{Pr}_{1-x}\text{Nd}_x)_2\text{Fe}_{14}\text{B}$  compounds has been measured by using the singular point detection (SPD) technique. The measured temperature and composition dependence of the anisotropy field has been compared with the data obtained in CEF approximations using different sets of  $\{A_n\}$  parameters for  $\text{Nd}_2\text{Fe}_{14}\text{B}$  and  $\text{Pr}_2\text{Fe}_{14}\text{B}$  and by considering a linear combination of the anisotropy in the mixed system. The comparison is made by calculating the anisotropy constants, then the anisotropy field values, starting from the  $\{A_n\}$  parameters. Experimental and calculated data concerning the occurrence of spin reorientation transition (SRT) and of type 1 and type 2 first-order magnetisation processes (FOMP) as a function of composition have also been compared.

### 1. Introduction

The intermetallic compounds  $\text{R}_2\text{Fe}_{14}\text{B}$  (R denotes a rare earth element) are the subject of extensive investigations in connection with high energy permanent magnets produced on the basis of  $\text{Nd}_2\text{Fe}_{14}\text{B}$  [1]. The  $\text{R}_2\text{Fe}_{14}\text{B}$  compounds have a tetragonal structure with space group  $\text{P4}_2/\text{mnm}$  [2]. The existence of different crystallographic sites for R and Fe ions and the interplay between intersublattice exchange and CEF interaction lead to the wide variety of the magnetic properties of this series of compounds [3–6].

In isostructural intermetallic compounds, with different R, the easy magnetisation direction is usually determined by the sign of the second-order crystal field parameter [7] which depends on the sign of the second-order Stevens coefficient  $\alpha_1$ . For  $\text{Pr}^{3+}$  and  $\text{Nd}^{3+}$  ions  $\alpha_1$  is negative, and both  $\text{Nd}_2\text{Fe}_{14}\text{B}$  and  $\text{Pr}_2\text{Fe}_{14}\text{B}$  present an easy  $c$  axis at room temperature. However when the temperature decreases a spin reorientation transition occurs at 135 K in  $\text{Nd}_2\text{Fe}_{14}\text{B}$  [8]. At 4.2 K the easy magnetisation direction lies in the plane [110] at an angle of  $\approx 30^\circ$  with respect to the  $c$  axis. On the other hand  $\text{Pr}_2\text{Fe}_{14}\text{B}$  remains easy  $c$  axis from 4.2 K to  $T_C$  [9]. In both compounds a first order magnetisation process (FOMP) has been observed. The FOMP is type 1 (after the transition the system is saturated) in  $\text{Nd}_2\text{Fe}_{14}\text{B}$  when the field is applied in the basal plane, along the [100] direction at  $T < 200$  K [10], whilst a type 2 FOMP (system not saturated after the transition) has been observed below 100 K in  $\text{Pr}_2\text{Fe}_{14}\text{B}$  with the field applied in the basal plane both along [100] and [110] directions [11]. Both fourth and sixth order CEF parameters or anisotropy constants are required in order to explain the observed phenomena and the different behaviour of Nd and Pr compounds.

However some contradictory data, on these systems, are still present in the recent literature: in some papers [12, 13] the anisotropy constants  $K_1$ ,  $K_2$  and  $K_3$  were deduced

from the measurements of magnetisation curves of aligned samples  $(\text{Pr}_{1-x}\text{Nd}_x)_2\text{Fe}_{14}\text{B}$ . In all cases, for both the extrema, a positive value of  $K_2$  was obtained. However, according to the theory of FOMP, a type 2 process in an easy axis system must be described by negative  $K_2$  [14].

Recently the spin structure and magnetisation curves of single crystals  $\text{R}_2\text{Fe}_{14}\text{B}$  were calculated using combined molecular-field and CEF approximations [15, 16]. On the basis of point charge calculations and Mössbauer spectroscopy data the set of CEF parameter  $\{A_n^m\}$  was determined which, following the authors, describe the observed magnetisation curves. For  $\text{Nd}_2\text{Fe}_{14}\text{B}$ , [15–17] used practically the same set of  $\{A_n^m\}$ . In the case of  $\text{Pr}_2\text{Fe}_{14}\text{B}$ , however, there are differences concerning not only the values, but also the sign of some CEF parameters. In addition it can be noted that the existence of difficulties in accounting for the observed magnetic properties of these systems were directly underlined by authors in [17, 18] and it is evident from the analysis of the data in [16]. In fact, in [18] the authors declare that CEF parameters deduced in the low-temperature range do not give a perfect account of the magnetisation curves above 150 K. To obtain a good agreement the values of the parameters were reduced by 15% at room temperature and no explanation was found for this. The authors in [17], referring to  $\text{Nd}_2\text{Fe}_{14}\text{B}$ , refined the CEF parameters for each case (i.e. at various temperatures) to reproduce the observed phenomena. They explained the necessity for this by the fact that crystal-field interactions are not negligible compared to the molecular-field interactions. However they obtained ratios of 15 and 5 between Nd and Fe anisotropies respectively at 4.2 K and room temperature (RT). The analysis of experimental data gives a ratio of 3.7 (–33%) at 293 K whilst the ratio of 15 is found to be practically correct at 4.2 K. In [16] it is evident from figures 10 and 11 that the calculated values of  $H_A$  at 290 K are about 30% larger than those measured in  $\text{Nd}_2\text{Fe}_{14}\text{B}$  and  $\text{Pr}_2\text{Fe}_{14}\text{B}$ . It is worth noting that in [17] and [18] the possibility of a canting between sublattice magnetisation was taken into account and that in [16] the effects of excited J multiplets were considered.

The exclusive single-ion origin of the anisotropy in both  $\text{Nd}_2\text{Fe}_{14}\text{B}$  is questioned in [19] where, from the analysis of experimental data it is inferred that a two-ion mechanism, connected with anisotropic exchange is responsible for the 45% of the anisotropy in this compound.

In the present work, the measurements of the temperature and composition dependence of the anisotropy field of pseudobinary  $(\text{Pr}_{1-x}\text{Nd}_x)_2\text{Fe}_{14}\text{B}$  compounds, performed by using the singular point detection (SPD) technique, are presented. With the aim of verifying if the R sublattice anisotropy has a pure crystal field origin (single ion) the values of the anisotropy field, measured at different temperatures and compositions, were compared with the values obtained in the CEF approximation using some available sets of  $\{A_n^m\}$  parameters for  $\text{Nd}_2\text{Fe}_{14}\text{B}$  and  $\text{Pr}_2\text{Fe}_{14}\text{B}$  and considering their linear combination for the mixed system. In order to calculate the anisotropy the following procedure was used: starting from the  $\{A_n^m\}$  parameters, the values of the corresponding anisotropy coefficients  $K_n^m$  at 0 K were derived (see equation (4)). Their temperature variation was obtained using the quantum analogy of the  $l(l+1)/2$  power law (see equations (5–8)). At any temperature it was thus possible to derive the values of the anisotropy constants of the R sublattice (3). After the addition of the phenomenological anisotropy constant of the Fe sublattice both the anisotropy field values (4) and the temperature of the SRT ( $K_1 = 0$ ) were calculated and compared with the experimental data for different compositions and temperatures ( $H_A$ ). The present phenomenological procedure to verify the origin of the magnetic anisotropy is based on the assumption that, in the case of single ion origin of the R anisotropy, both a linear dependence of the

**Table 1.** Lattice constants and anisotropy field at 293 K and  $T_{SR}$  of  $(Pr_{1-x}Nd_x)_2Fe_{14}B$ .

$x$	$a$ (Å)	$c$ (Å)	$H_A$ (kOe) ( $T = 293$ K)	$T_{SR}$ (K)
0	8.813	12.255	87.7	—
0.2	8.812	12.255	89.3	—
0.4	8.812	12.249	88.5	50 <sup>†</sup>
0.6	8.811	12.239	86.9	86
0.8	8.811	12.230	86.3	112
1	8.809	12.225	82.5	135

<sup>†</sup> Extrapolated value.

anisotropy on composition and a temperature dependence following the  $l(l+1)/2$  power law are expected to be valid [20].

This approach was chosen because the calculation of  $H_A$  and the evaluation of the SRT are very simple when done using the anisotropy constants. Furthermore experimental and calculated data concerning the occurrence of type 1 and type 2 FOMP, such as the composition dependence of the onset temperature and the critical field values can be easily compared using the phenomenological description.

## 2. Experimental details and results

A series of  $(Pr_{1-x}Nd_x)_2Fe_{14}B$  compounds with  $x = 0, 0.2, 0.4, 0.6, 0.8$  and  $1.0$  were prepared by melting the constituents under argon atmosphere in an induction furnace. All ingots were annealed at  $1100^\circ\text{C}$  in argon gas for 10 h. X-ray diffraction, metallographic analysis and TMA showed that all the samples were essentially single phase with no more than 3% of  $\alpha$ -Fe phase. The lattice constants of all compounds are listed in table 1.

The anisotropy ( $H_A$ ) and critical field of the FOMP ( $H_{CR}$ ) were measured as a function of temperature and composition by using the SPD technique [21] in oriented powder specimens. The shape of observed SPD signals at 77 K are shown in figure 1. The difference between the SPD signals of  $Nd_2Fe_{14}B$  and  $Pr_2Fe_{14}B$  are associated with the different types of FOMP present in Pr and Nd compounds. It can be seen that all compounds except  $(Pr_{0.8}Nd_{0.2})_2Fe_{14}B$  display a FOMP at 77 K. A type 1 process is observed for  $x = 1, 0.8, 0.6, 0.4$  whilst a type 2 FOMP is observed in  $Pr_2Fe_{14}B$ . The FOMP onset temperature was found to decrease with increasing Pr content from  $T \approx 220$  K for  $x = 1$  to  $T \approx 160$  K for  $x = 0.4$ . The temperature dependence of the critical field of the transition is reported in figure 2(a). On the other hand the SPD signal of all compounds at room temperature is typical of an easy  $c$  axis ferromagnet. The temperature dependences of the anisotropy fields  $H_A$  are shown in figure 2(b). At room temperature an 8% variation in the  $H_A$  values is observed along the series (see table 1). As the temperature decreases, however,  $H_A$  in  $Pr_2Fe_{14}B$  increases more rapidly than in  $Nd_2Fe_{14}B$ . It is worth noting that due to the experimental conditions, as usual, only one of the two expected peaks relative to the two hard directions in the basal plane [100] and [110], was detected in the SPD spectrum. This peak corresponds to the lower field value which is  $H_A$  (or  $H_{CR}$ ) along [100] for both  $Pr_2Fe_{14}B$  [11] and  $Nd_2Fe_{14}B$  [10] even if in the latter case the direction [100] corresponds to the hard direction in the basal plane.

The temperature of the spin reorientation transition axis to a cone, which takes place at 135 K in  $Nd_2Fe_{14}B$ , decreases linearly with increasing Pr content (see table 1).  $T_{SR}$

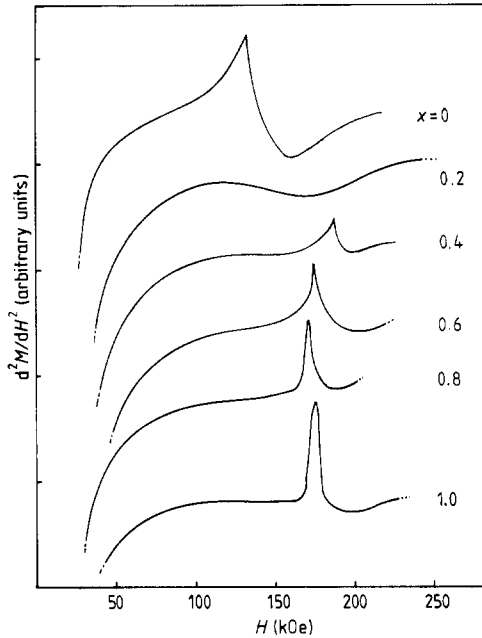


**Figure 1.** SPD signals  $d^2M/dH^2$  against  $H$  at 77 K from various sample compositions in  $(Pr_{1-x}Nd_x)_2Fe_{14}B$ .

was determined by measuring the initial susceptibility of oriented powder specimens in a magnetic field of 50 Oe.

In the next paragraph a description of the observed phenomena in terms of anisotropy constants, calculated from CEF parameters, will be given.

### 3. Analysis

The usual phenomenological expression for the anisotropy energy of a tetragonal system, in terms of anisotropy constants, is:

$$E_A = K_1 \sin^2 \theta + (K_2 + K'_2 \cos 4\varphi) \sin^4 \theta + (K_3 + K'_3 \cos 4\varphi) \sin^6 \theta + \dots \quad (1)$$

where  $\theta$  is the angle between the magnetisation vector  $M_S$  and the  $c$  axis,  $\varphi$  is the angle between the projection of  $M_S$  in the basal plane and the  $[100]$  direction. An alternative expression for  $E_A$  is that in terms of anisotropy coefficients using the orthonormal Legendre polynomials:

$$E_A = \sum_{n,m} K_n^m P_n^m(\cos \theta) \cos m\varphi \\ = k_2^0 P_2^0 + k_4^0 P_4^0 + k_6^0 P_6^0 + (k_4^4 P_4^4 + k_6^4 P_6^4) \cos 4\varphi. \quad (2)$$

There is a simple relationship between anisotropy constants  $K_i$  in (1) and anisotropy coefficients  $k_n^m$  in (2) [22]:

$$K_1 = -\left[\frac{3}{2}k_2^0 + 5k_4^0 + \frac{21}{2}k_6^0\right] \quad K'_2 = \frac{1}{8}[k_4^4 + 5k_6^4] \\ K_2 = \frac{7}{8}[5k_4^0 + 27k_6^0] \quad K'_3 = -\frac{11}{16}k_6^4. \quad (3) \\ K_3 = -\frac{231}{16}k_6^0$$

In such a phenomenological description the anisotropy constants (or coefficients) are relative to the overall anisotropy.

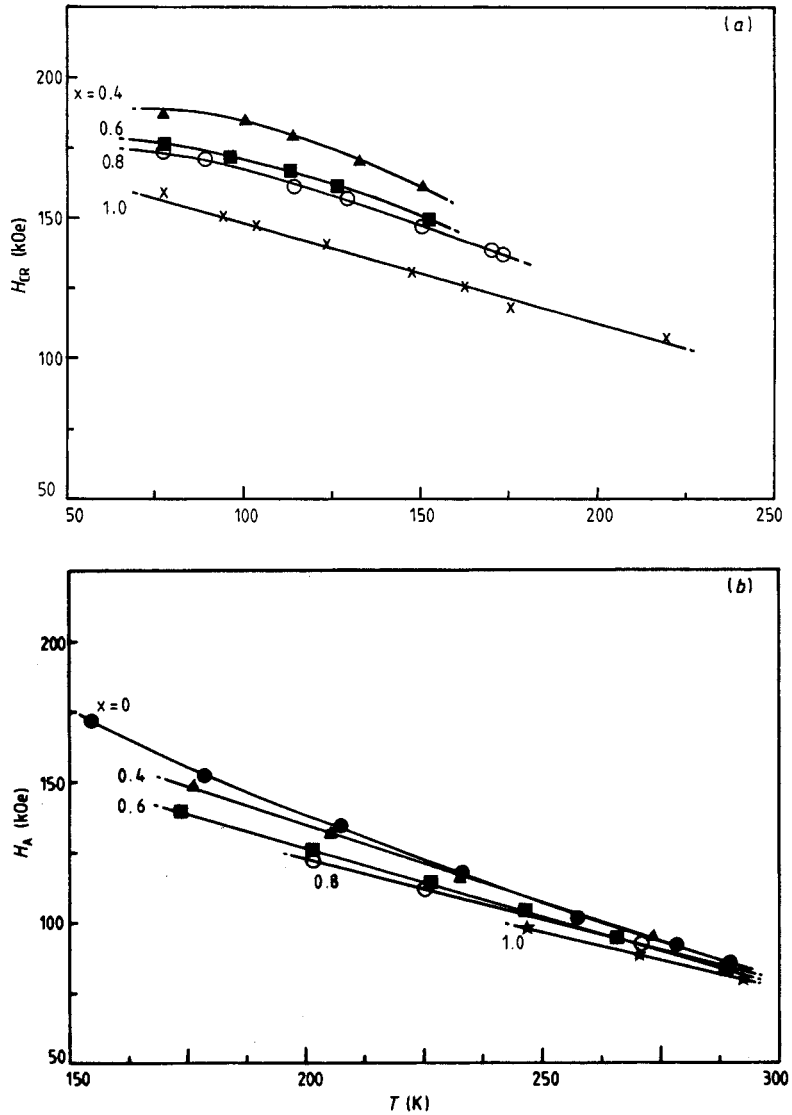


**Figure 2.** (a) Temperature and composition dependence of the critical field  $H_{CR}$  in  $(Pr_{1-x}Nd_x)_2Fe_{14}B$ . (b) Temperature and composition dependence of the anisotropy field  $H_A$  in  $(Pr_{1-x}Nd_x)_2Fe_{14}B$ .

In the case in which the exchange energy of Fe-R is much larger than the CEF potentials energy of the R ion, Legendre polynomials are classical equivalents of Stevens operators. Therefore at 0 K the coefficients  $k_n^m$  are connected directly to the CEF parameters [16, 23–25]:

$$k_n^m = B_n^m \langle O_n^0 \rangle = \Theta_n \langle r_0^n \rangle \langle O_n^0 \rangle A_n^m \quad (4)$$

where  $\Theta_2 = \alpha_J$ ,  $\Theta_4 = \beta_J$ ,  $\Theta_6 = \gamma_J$  are Stevens parameters,  $\langle r_0^n \rangle$  is the average of the  $n$ th power of the 4f shell radius calculated respectively in [26] and [27],  $\langle O_n^0 \rangle$  are the expectation values of Stevens equivalent operators tabulated in [26];  $A_n^m$  are the CEF

parameters, being

$$H_{\text{CEF}} = \sum_{n,m} B_n^m O_n^m$$

the Hamiltonian which describes the CEF interactions of R ions, in the ground J multiplet. It should be emphasised that the anisotropy coefficients, as derived from (4), describe the rare earth sublattice anisotropy.

The temperature dependence of the anisotropy coefficients  $k_n^m$ , obtained by (4) at 0 K, can be determined either by using the functions  $L_n(x) = k_n^0(T)/k_n^0(0)$  described in [25] or by directly using the  $l(l+1)/2$  power law, which was shown to be valid in almost all the ferromagnetic range, in the case of single-ion anisotropy [20].  $L_n(x)$  functions are the quantum analogues of hyperbolic Bessel functions, which are used in the Callen and Callen theory [20].

In the molecular-field approximation, for a two sublattices ferromagnet, the argument of the  $L_n(x)$  functions is:

$$X(T) = [g_J \mu_B J H_m(T)] / K_B T \quad (5)$$

where  $H_m(T)$  is the molecular field due to the Fe sublattice acting on the total moment  $J$  of the R ions. It is reasonable to assume that Fe–R exchange interaction does not affect the Fe sublattice magnetisation and that R–R interaction can be neglected, thus the temperature dependence of  $H_m$  is given by:

$$H_m(T) = H_m(0) \sigma_{\text{Fe}}^*(T) \quad (6)$$

where  $\sigma_{\text{Fe}}^*(T) = \sigma_{\text{Fe}}(T)/\sigma_{\text{Fe}}(0)$  is the reduced magnetisation of Fe sublattice and can be deduced from the data of  $\text{Y}_2\text{Fe}_{14}\text{B}$ . The intersublattice molecular-field parameter is defined as:

$$\xi_0 = [g_J \mu_B J H_m(0)] / K_B \quad (7)$$

thus

$$X(T) = [\xi_0 \sigma_{\text{Fe}}^*(T)] / T. \quad (8)$$

Using the values of the crystal field parameters at 0 K taken from [15–17], the temperature dependence of Fe sublattice magnetisation as in  $\text{Y}_2\text{Fe}_{14}\text{B}$  [28] and molecular-field parameters taken both from [15, 16], we calculated the values of the anisotropy coefficients  $k_n^m$  at 0 K (using (4)) and their temperature dependence. In order to compare experimental and calculated data of the  $(R'_{1-x}R''_x)_2\text{Fe}_{14}\text{B}$  pseudobinary system, the assumption that the resultant anisotropy is a linear combination of  $\text{Nd}_2\text{Fe}_{14}\text{B}$  and  $\text{Pr}_2\text{Fe}_{14}\text{B}$  contributions was made, that is:

$$(k_n^m)_{\text{Pr}_{(1-x)}\text{Nd}_x\text{Fe}_{14}\text{B}} = (k_n^m)_{\text{Nd}_2\text{Fe}_{14}\text{B}} X + (k_n^m)_{\text{Pr}_2\text{Fe}_{14}\text{B}} (1 - X) \quad (9)$$

which can be considered a reasonable approximation in the case of a single-ion origin of the R sublattice anisotropy.

In order to calculate the temperature dependence of the coefficients  $k_n^m$ , using the power law directly, the R sublattice magnetisation was obtained by subtracting the magnetisation of the  $\text{Y}_2\text{Fe}_{14}\text{B}$  compound from the overall saturation magnetisation.

The anisotropy constants were obtained from anisotropy coefficients using (3) and the anisotropy field values were calculated using the expression:

$$H_A = [2K_1 + 4(K_2 \pm K'_2) + 6(K_3 \pm K'_3)] / M_S \quad (10)$$

where the – and + sign refer to the [110] ( $\varphi = 45^\circ$ ) and [100] ( $\varphi = 0^\circ$ ) directions

**Table 2.** Calculated anisotropy coefficients  $k_n^m$  calculated from crystal field parameters  $A_n^m$  of [15] (a) and [16] (b) for  $Nd_2Fe_{14}B$  and  $Pr_2Fe_{14}B$ . The values of the molecular field parameter  $\xi_0$  have been obtained from the best fit of the anisotropy field value  $H_A = (2K_2 + 4K_2 + \dots)/M_5$  at 293 K. The values in parentheses are those given in [15] (a) and [16] (b).

		Pr			Nd		
<i>n</i>	<i>m</i>	$A_n^m$ ( $Ka_0^{-n}$ )	$k_n^m$ ( $K/\text{ion}$ )	$k_n^m$ ( $10^7 \text{ erg cm}^{-3}$ )	$A_n^m$ ( $Ka_0^{-n}$ )	$k_n^m$ ( $K/\text{ion}$ )	$k_n^m$ ( $10^7 \text{ erg cm}^{-3}$ )
(a)							
2	0	+177.5	-126.56	-14.14	+306	-78.95	-8.86
4	0	+3	-6.36	-0.71	-14	+17.93	+2.01
6	0	-7	-41.25	-4.61	-2	+17.33	+1.95
4	4	-1	+2.1	+0.23	+2	-2.56	-0.29
6	4	-23	-135.54	-15.54	-23	+199.25	+22.37
$\xi_0$ [K]		465 (452)			634 (669)		
(b)							
2	0	+295	-210.34	-23.5	+295	-76.11	-8.54
4	0	-12.3	+26.09	+2.91	-12.3	+15.76	+1.77
6	0	-6.89	-40.6	-4.54	-1.84	+15.94	+1.79
4	4	0	0	0	0	0	0
6	4	-29.8	-175.61	-19.62	-15.9	+137.74	+15.46
$\xi_0$ [K]		342 (480)			651 (725)		

respectively.  $K_1$  is actually the overall second-order anisotropy term obtained by the addition of that calculated for the R sublattice and the experimental Fe sublattice anisotropy. For the Fe sublattice an average of the  $K_1$  values of  $Y_2Fe_{14}B$  and  $La_2Fe_{14}B$  was used [6]. Due to the fact that this calculation, performed using the  $\xi_0$  parameter given in [15] or [16], gave for  $H_A$  at 293 K values which were 30–40% larger than that measured (see below), alternative values for  $\xi_0$ , which gave the correct values of  $H_A$  at RT for both  $Nd_2Fe_{14}B$  and  $Pr_2Fe_{14}B$ , were also considered (see table 2).

#### 4. Discussion

Comparison of the experimental data with the results of calculations show that both the sets of CEF parameters used account for, at least qualitatively, the presence and behaviour of FOMP in the pseudobinary  $(Pr_{1-x}Nd_x)_2Fe_{14}B$ . In figures 3 and 4 the representative lines for the compositions of the various samples in terms of reduced anisotropy constants are reported on a particular zone of the FOMP phase diagrams reproduced from [14]. These lines correspond to the temperature variation of the anisotropy constant ratios  $K_2^{\text{eff}}/K_1 = x$  and  $K_3^{\text{eff}}/K_1 = y$ . The expression  $K^{\text{eff}}$  indicates that fourth and sixth order anisotropy constants contain the planar contributions  $K_2'$  and  $K_3'$  respectively (see (1)).

In particular figure 3 refers to the [100] direction whilst figure 4 refers to the [110] direction. The results shown are obtained from the data of [16] using the  $\xi_0$  deduced from the best fit of the  $H_A$  value at 293 K (similar results are obtained with the parameters and  $\xi_0$  of [15] or [17] for the Nd system). The onset of FOMP is evidenced by the crossing of the lines  $u$  and  $t$  for type 1 and type 2 process respectively. Considering the [100] direction, present calculations evidence the occurrence of type 1 FOMP in  $(Pr_{1-x}Nd_x)_2Fe_{14}B$  for  $x = 1, 0.8, 0.6$ . However, in contradiction to SPD measurements, no FOMP is expected for  $x = 0.4$  (figures 1 and 3). A type 2 FOMP is predicted for  $x = 0$  and 0.2 along [100]. However no FOMP is observed for  $x = 0.2$  by SPD down to 77 K



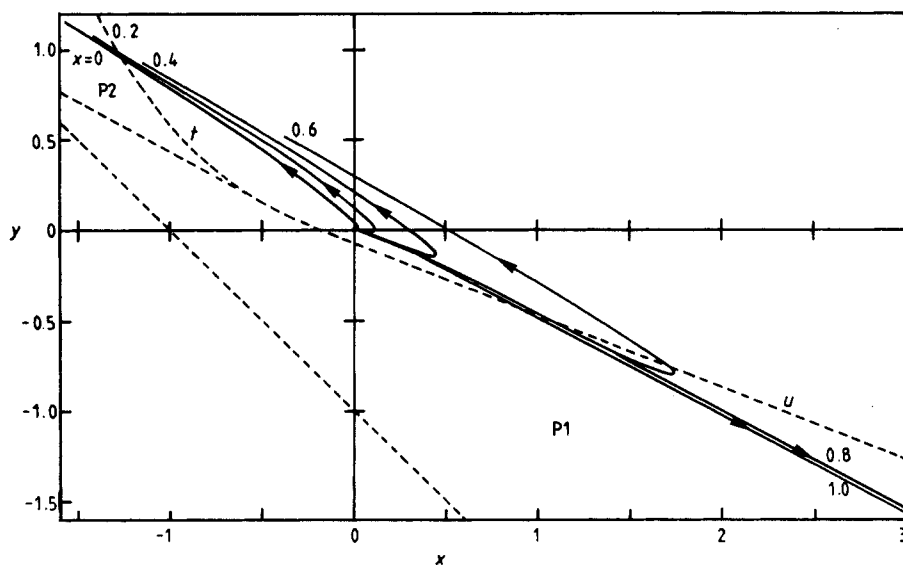


**Figure 3.** Representative lines for different compositions of  $(\text{Pr}_{1-x}\text{Nd}_x)_2\text{Fe}_{14}\text{B}$  in the diagram of FOMP, in terms of reduced anisotropy constants ( $x = (K_2 + K'_2)/K_1$ ;  $y = (K_3 + K'_3)/K_1$ ) deduced for the [100] direction in the basal plane. The arrows indicate the direction to be followed when the temperature decreases. These values have been calculated from CEF parameters given in [16].

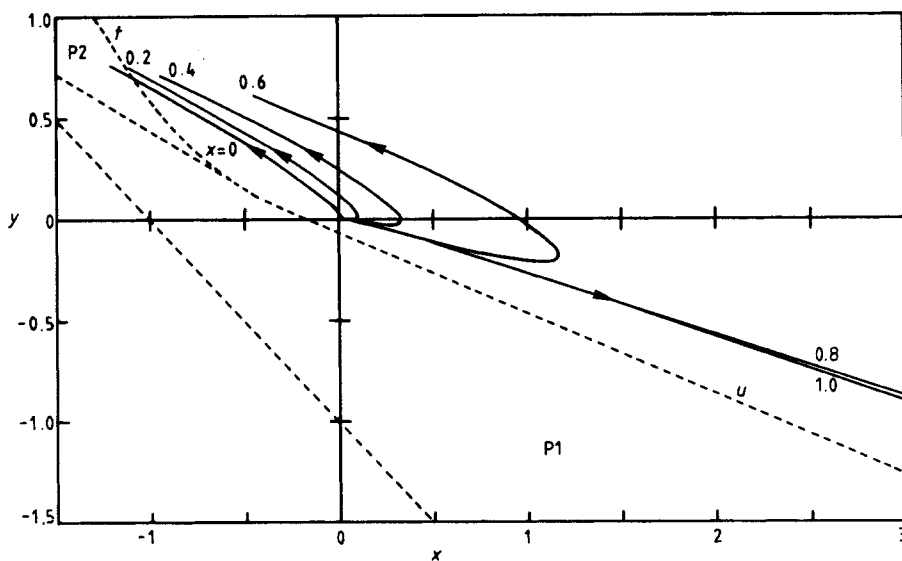


**Figure 4.** Representative lines for different compositions of  $(\text{Pr}_{1-x}\text{Nd}_x)_2\text{Fe}_{14}\text{B}$  in the diagram of FOMP in terms of reduced anisotropy constants ( $x = (K_2 - K'_2)/K_1$ ;  $y = (K_3 - K'_3)/K_1$ ) deduced for the [110] direction in the basal plane. The arrows indicate the direction followed when the temperature decreases. These values have been calculated from CEF parameters given in [16].

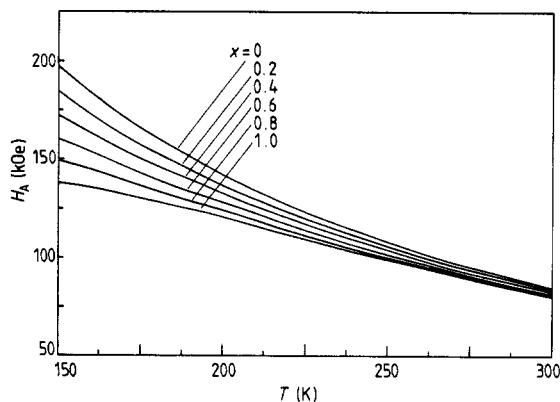


**Figure 5.** Temperature dependence of the calculated anisotropy field values (from data of [15]) in  $(Pr_{1-x}Nd_x)_2Fe_{14}B$  for the [100] direction in the basal plane.

(figure 1). Along [110] the type 2 FOMP is predicted to occur only in  $Pr_2Fe_{14}B$  (figure 4). In conclusion some disagreement between the experiments and calculations is evident in the composition range  $0.2 \leq x \leq 0.4$ , that is in the Pr-rich region.

Comparing the temperature dependence of the measured (figure 2(b)) and calculated values of  $H_A$  along [100] from data of [15] (figure 5) it is evident that there is a substantial agreement for  $x \geq 0.4$  down to 150 K, however some problems are evident in the Pr-rich side particularly when data from [16] are used; in fact the calculated temperature dependence of  $H_A$  is much steeper than that measured. The presence of the FOMP does not allow for the analysis of  $H_A$  (along [100]) below 150 K.

The difficulties encountered in describing Pr-rich systems could be connected with the fact that for Pr the assumed condition that R-Fe exchange energy is much larger than the CEF potential energy is not true. In this instance, as noted in [29], the analytical expression of the anisotropy coefficients in terms of CEF parameters (4) is no longer valid, thus justifying the progressive disagreement between calculated and experimental data with increasing Pr content. An alternative explanation of the observed difficulty can be that the anisotropy given by Pr ions is not purely single-ion in origin.

Using the values of the molecular-field and CEF parameters given in [15] and [16] the right value of  $T_{SR}$  was obtained for the series (expressed as the temperature at which  $K_1 = 0$ ). However a value for  $H_A$  at RT is obtained which is 30–40% larger than that measured in both Nd and Pr compounds ( $H_A = 82.5$  kOe for Nd and  $H_A = 87.7$  kOe for Pr). On the other hand, by using  $\xi_0$  values deduced from the best fit of  $H_A$  at 293 K together with the CEF parameters given in [15–17], an incorrect description of the low-temperature SRT is found. As is evident from data in figure 6, a SRT is predicted only for  $Nd_2Fe_{14}B$  at  $T_{SR} = 90$  K. However such a reorientation transition temperature is about 40 K lower (–34%) than that observed. In addition, contrary to the prediction, a SRT axis to a cone has been found experimentally, at 112 K and 86 K, for  $x = 0.8$  and 0.6 respectively (table 1).

In conclusion it was not possible to find any value of the parameter  $\xi_0$  which could simultaneously give the correct values of the room temperature anisotropy field and of  $T_{SR}$ . It was also not possible to describe correctly both the high and low temperature anisotropy of the system at the same time.

It must be admitted that actual sets of CEF parameters [15–17], which express the single-ion anisotropy of the system, give a good general qualitative account of the various

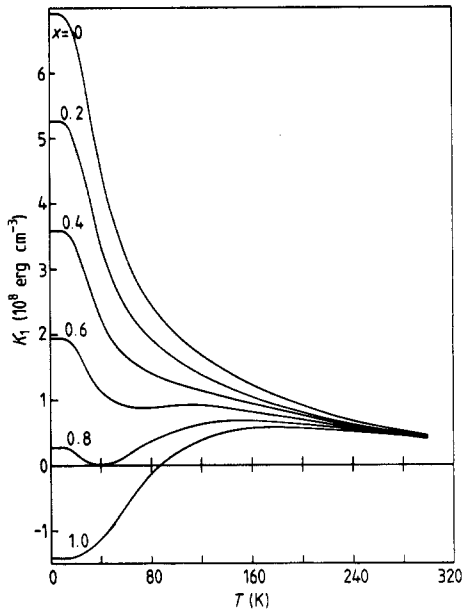


**Figure 6.** Temperature dependence of the calculated anisotropy constant  $K_1$  (from data of [16]) in  $(\text{Pr}_{1-x}\text{Nd}_x)_2\text{Fe}_{14}\text{B}$ .

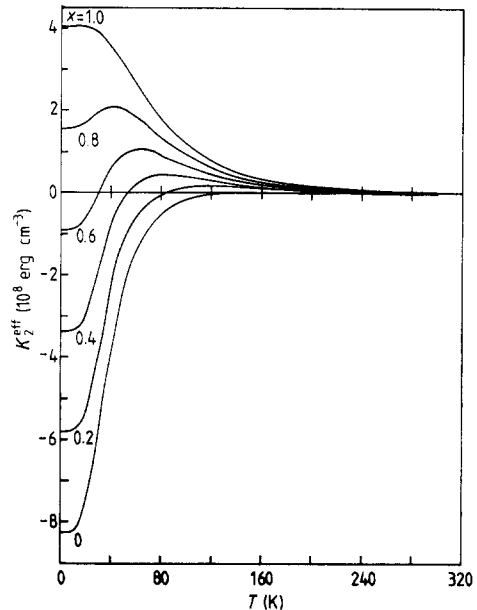


**Figure 7.** Temperature dependence of the calculated anisotropy constant  $K_2^{\text{eff}} = K_2 - K_2'$  (from data of [16]) in  $(\text{Pr}_{1-x}\text{Nd}_x)_2\text{Fe}_{14}\text{B}$ .

magnetic processes ( $H_A$ , FOMP, SRT). However, the quantitative agreement is only partial; in fact in accounting for the  $T_{\text{SR}}$  value an incorrect value of the room temperature anisotropy field value is obtained and, *vice versa*, in accounting for the right  $H_A$  value, an incorrect  $T_{\text{SR}}$  is found, furthermore no completely correct predictions of the occurrence of FOMP as function of composition are obtained. We recall that similar difficulties were also expressed in [16–18]. Previous results seem to indicate that something has been neglected concerning the origin of the anisotropy of these compounds. A non-negligible contribution to the anisotropy coming from the presence of an anisotropic exchange energy could explain the partial failure of the previous analysis concerning magnetic phenomena connected with the magnetocrystalline anisotropy in 2:14:1 intermetallic compounds.

The observed difficulty in describing the anisotropy of the R sublattice in terms of only a single-ion contribution is also directly evident from the phenomenological analysis performed in  $\text{Nd}_2\text{Fe}_{14}\text{B}$  single-crystal magnetisation curves [10] in terms of anisotropy constants. Such an analysis gives the effective overall anisotropy constants of the system, irrespective of the origin of the various anisotropy contributions. The set of  $K_n$  given in [10] and obtained from the fit of the experimental magnetisation curves, using the phenomenological expression (1), accounts for all the features (anisotropy, FOMP, SRT) observed in  $\text{Nd}_2\text{Fe}_{14}\text{B}$ . Starting from this set of anisotropy constants  $K_n$ , after the subtraction of the Fe contribution ( $K_1$  of  $\text{Y}_2\text{Fe}_{14}\text{B}$ ), the anisotropy coefficients  $k_n^m$  of the R sublattice were calculated by inverting (3). Making this operation for the  $K_n$  values, for instance, at 150 K, it is expected that, in the presence of only single-ion anisotropy, the application of the power  $l(l+1)/2$  law for the temperature variation of the  $k_n^m$  coefficients would allow us to obtain the correct values of the anisotropy constants at any temperature. This hypothesis was not verified even taking into account a possible

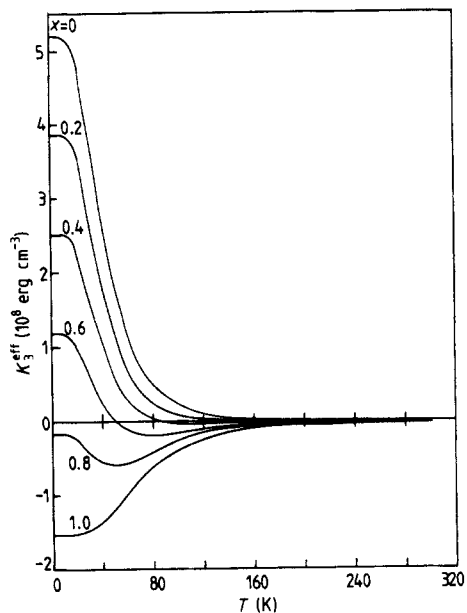


**Figure 8.** Temperature dependence of the calculated anisotropy constant  $K_3^{\text{eff}} = K_3 - K_3'$  (from data of [16]) in  $(Pr_{1-x}Nd_x)_2Fe_{14}B$ .

modification of the  $K_n$  values which could originate from the presence of different contributions to the magnetic anisotropy [30–34].

This analysis further supports the hypothesis that the R sublattice anisotropy cannot be accounted for with crystal field arguments only, that is R anisotropy has not a pure single-ion origin. A two-ion mechanism, connected with an anisotropic exchange can have a relevant part in the formation of the magnetic anisotropy in R intermetallic systems.

As a marginal result of the present analysis it can be observed that the phenomenological description of the anisotropy in terms of anisotropy constants proves to be much more sensitive to the variation of the magnetic characteristics than that in terms of anisotropy coefficients  $k_n^m$  or CEF parameters  $\{A_n^m\}$ . In fact, besides  $K_1$ , which is positive for Pr and negative for Nd at low temperature, both the high order anisotropy constants  $K_2$  and  $K_3$ , as obtained from data from [16], invert their sign when changing composition from  $Nd_2Fe_{14}B$  to  $Pr_2Fe_{14}B$  (see figures 6, 7, 8). This is a generally expected feature if a change from a type 1 to a type 2 FOMP takes place [14]. On the other hand in the CEF parameters description the different properties of  $Pr_2Fe_{14}B$  and  $Nd_2Fe_{14}B$  compounds are simply qualified by different signs of the  $B_6^0$  coefficients in the two systems. For instance, considering the occurrence of the SRT, the analysis of:

$$K_1 = -\left(\frac{3}{2}B_2^0\langle O_n^0 \rangle + 5B_4^0\langle O_4^0 \rangle + \frac{1}{2}B_6^0\langle O_6^0 \rangle\right) \quad (11)$$

where  $B_6^0 = \gamma_J \langle r^6 \rangle A_6^0$ ,  $\gamma_J > 0$  for Pr and  $\gamma_J < 0$  for Nd indicate that it is the positive term  $B_6^0$  which permits the occurrence of a change in sign of  $K_1$  (thus a SRT) in  $Nd_2Fe_{14}B$  ( $B_2^0$  and  $B_4^0$  are negative in both systems). Furthermore the positive  $B_6^0$  favours the occurrence of type 1 FOMP in  $Nd_2Fe_{14}B$  whilst when negative it determines, in conjunction with a negative  $B_4^0$  term, the occurrence of a type 2 FOMP in  $Pr_2Fe_{14}B$ .

## References

- [1] Sagawa M, Fujimura S, Togawa N, Yamamoto H and Matsuura Y 1984 *J. Appl. Phys.* **55** 2083
- [2] Herbst J F, Croat J J, Pinkerton F E and Yelon W B 1984 *Phys. Rev. B* **29** 4176

- [3] Hiroswawa S, Matsuura Y, Yamamoto H, Fujimura S, Sagawa M and Yamauchi H 1986 *J. Appl. Phys.* **59** 873
- [4] Koon N C, Das B N, Rubinstein M and Tyson J 1985 *J. Appl. Phys.* **57** 4091
- [5] Pareti L, Bolzoni F and Moze O 1985 *Phys. Rev. B* **32** 7604
- [6] Pareti L, Solzi M, Bolzoni F, Moze O and Panizzieri R 1987 *Solid State Commun.* **61** 761
- [7] Greedan J E and Rao V U S 1973 *J. Solid State Chem.* **6** 387
- [8] Givord D, Li H S and de la Bathie Perrier R 1984 *Solid State Commun.* **51** 857
- [9] Hiroyoshi H, Saito N, Kido G, Nakagawa Y, Hiroswawa S and Sagawa M 1986 *J. Magn. Magn. Mater.* **54-57** 583
- [10] Bolzoni F, Moze O and Pareti L 1987 *J. Appl. Phys.* **62** 615
- [11] Hiroyoshi H, Kato H, Yamada M, Yamada M, Saito N, Nakagawa Y, Hiroswawa S and Sagawa M 1987 *Solid State Commun.* **62** 475
- [12] Ying-Kai Huang, Wu C H, Chuang Y C, Fu-Ming Y and de Boer F R 1987 *J. Less-Common Met.* **132** 317
- [13] Yang Y-C, James W J, Chen H-Y and Sun H 1986 *J. Magn. Magn. Mater.* **54-57** 895
- [14] Asti G and Bolzoni F 1980 *J. Magn. Magn. Mater.* **20** 29
- [15] Coey J M D, Li H S, Gavigan J P, Cadogan J M and Hu B P 1988 *Final report Concerted European Action on Magnets (CEAM)* Madrid 203
- [16] Yamada M, Kato H, Yamamoto H and Nakagawa Y 1988 *Phys. Rev. B* **38** 620
- [17] Radwanski R J and Franse J J M 1989 *J. Magn. Magn. Mater.* **80** 14
- [18] Cadogan J M, Gavigan J P, Givord D and Li H S 1988 *J. Phys. F: Met. Phys.* **18** 779
- [19] Kapusta Cz, Figiel H and Kakol Z 1990 *J. Magn. Magn. Mater.* at press
- [20] Callen H B and Callen E 1966 *J. Phys. Chem. Solids* **27** 1271
- [21] Asti G and Rinaldi S 1974 *J. Appl. Phys.* **45** 3600
- [22] Birss R R and Keeler G J 1974 *Phys. Status Solidi* **64** 357
- [23] Radwanski R J and Franse J J M 1988 *J. Magn. Magn. Mater.* **74** 43
- [24] Gavigan J P 1988 *PhD Thesis* Trinity College, Dublin
- [25] Kazakov A A and Andreeva R I 1970 *Sov. Phys.-Solid State* **12** 192
- [26] Hutchings M T 1964 *Advances in Research and Applications (Solid State Physics vol 16)* (New York: Academic)
- [27] Freeman A J and Desclaux J P 1979 *J. Magn. Magn. Mater.* **12** 11
- [28] Bolzoni F, Gavigan J P, Givord D, Li H S, Moze O and Pareti L 1987 *J. Magn. Magn. Mater.* **66** 158
- [29] Radwanski R J and Franse J J M 1987 *Phys. Rev. B* **36** 8616
- [30] Rinaldi S and Pareti L 1979 *J. Appl. Phys.* **50** 7719
- [31] Radwanski R J, Franse J J M and Sinnema S 1987 *J. Magn. Magn. Mater.* **70** 313
- [32] Sarkis A and Callen E 1982 *Phys. Rev. B* **26** 3870
- [33] Pareti L 1988 *J. Physique Coll.* **8 49** 551
- [34] Asti G, Bolzoni F and Pareti L 1987 *IEEE Trans. Magn.* **MAG-23** 2521